Atom Indonesia

Journal homepage: http://atomindonesia.brin.go.id

Analysis of Boron Neutron Capture Therapy Dose Rate for Head and Neck Rhabdomyosarcoma Cancer in a 10-Year-Old Child Phantom

E. Hidayanto, F. M. Salim, W. Setiabudi, F. Arianto*

Department of Physics, Faculty of Science and Mathematics, Diponegoro University, Semarang, Indonesia.

ARTICLE INFO

Article history:
Received 22 May 2025
Received in revised form 31 October 2025
Accepted 27 November 2025

Keywords:

Absorbed dose
BNCT
Head and neck rhabdomyosarcoma
Monte Carlo
MCNP 6.2

ABSTRACT

Rhabdomyosarcoma is a malignant cancer that affects soft tissues and predominantly occurs in children. Approximately 35–40% of cases occur in the head and neck region. Boron Neutron Capture Therapy (BNCT) has been employed in the treatment of head and neck cancers and has shown promising results. However, neutron, proton, and gamma-ray scattering pose significant challenges, as they contribute to the total BNCT dose. This study aims to analyze the BNCT dose received by a 10-year-old child phantom. The method involves simulating an ORNL-MIRD head and neck phantom of a 10-year-old child irradiated with BNCT using the Monte Carlo N-Particle (MCNP) version 6.2 code. The BNCT dose was determined by calculating the absorbed dose, and the simulation results were analyzed based on the deterministic effects on at-risk organs. The absorbed dose values for the skin, brain, spinal cord, and thyroid were 0.00641 Gy, 1.566 Gy, 0.710 Gy, and 0.018 Gy, respectively. The deterministic effects on the skin and thyroid were minimal, as the absorbed doses did not exceed their respective threshold limits.

INTRODUCTION

Cancer is caused by abnormal tissue growth that develops rapidly, uncontrollably, and divides continuously [1]. One type of cancer that affects humans is Rhabdomyosarcoma (RMS). RMS is a malignant tumor that affects soft tissues and is most commonly found in children. RMS accounts for approximately 5% of all malignant tumors in children and 20% of all soft tissue malignancies [2]. The disease most frequently occurs in the head and neck region (35-40%), followed by the urogenital system, extremities, and trunk [3].

In Indonesia, 30 children diagnosed with RMS were treated at Dr. Hasan Sadikin General Hospital in Bandung between 2015 and 2018. Among these cases, 40% involved the head and neck region, and more than 80% of patients presented with advanced-stage disease. Of the 27 patients who received therapy, the majority (83%) underwent chemotherapy, while a smaller proportion received a combination of surgery or radiotherapy and three patients died before receiving treatment [4].

Based on the clinical study [4], most pediatric RMS patients in Indonesia presented with advanced-stage disease characterized by large tumors (>5 cm) and were primarily treated with single-modality chemotherapy due to limited access to alternative treatment options. Because RMS tumors predominantly occur in the head and neck region, and most patients are children in their growth phase, conventional surgery and radiotherapy pose a high risk of damaging surrounding organs. This condition highlights the need for a more selective, effective, and minimally invasive therapeutic approach, such as Boron Neutron Capture Therapy (BNCT), which is capable of delivering high radiation doses to cancer cells while minimizing exposure to surrounding normal tissues.

Boron Neutron Capture Therapy (BNCT) is an emerging radiotherapy technique designed to improve cancer control while minimizing damage to normal tissues. The BNCT procedure involves administering a boron-containing compound that selectively accumulates in cancer cells, followed by

*Corresponding author.
E-mail address: fajararianto@fisika.fsm.undip.ac.id
DOI:

irradiation of the tumor site with epithermal neutrons [5]. When the ^{10}B isotope captures a neutron, it forms ^{11}B and undergoes a neutron capture reaction followed by particle emission that produces high LET particles, including alpha particles (^{4}He), lithium nuclei (^{7}Li), as well as accompanying gamma rays. These particles can penetrate tumor cells and damage their DNA and/or RNA, ultimately leading to cell destruction [6]. BNCT has been widely applied and has demonstrated promising outcomes in the treatment of head and neck cancers [7].

Dosimetric calculations in BNCT include several main components of the absorbed dose: the boron (alpha) dose, nitrogen (proton) dose, gamma dose, and neutron dose, each contributing differently to the total dose absorbed by the tissue [8]. The absorbed dose received by tissues can induce deterministic effects, depending on factors such as exposure time, dose level, and radiation type. Deterministic effects are biological responses whose severity increases with the absorbed dose [9].

Dose analysis in BNCT is complex because it involves various types of radiation generated from neutron interactions with biological tissues. When tissues are exposed to epithermal neutron beams, the neutrons gradually slow down and become thermal neutrons within the tissue, resulting in a mixture of secondary radiations such as charged particles (α particles and protons), photons, and recoil neutrons, each possessing different biological effectiveness [10].

The spatial distribution of each dose component particularly the boron dose, gamma dose, and fast neutron dose is strongly influenced by the characteristics of the beam and the irradiation geometry within the irradiated volume. Therefore, accurate dose analysis using Monte Carlo simulations is a crucial step in evaluating the contribution of each component to the total dose and ensuring adequate protection of healthy tissues surrounding the target area.

The Monte Carlo N-Particle (MCNP) code is a computational tool that applies the Monte Carlo method to simulate the transport of neutrons, photons, and electrons in three-dimensional materials [11]. MCNP version 6.2, released in 2018, features enhanced physics models for secondary emission and decay production, decay sources, and cosmic rays. This version is capable of performing calculations approximately 1.5 to 2 times faster than its predecessors [12].

The study reported in Syamputra et al. (2018) was among the early investigations that highlighted the potential application of BNCT for rhabdomyosarcoma in the head and neck region of a 5-year-old child [13]. The research employed a Monte Carlo simulation approach using the PHITS code to calculate neutron flux distributions and dose rates in target tissues, which served as the basis for BNCT dose estimation. The results demonstrated that BNCT was capable of delivering high doses to the tumor region while maintaining low doses to surrounding head and neck organs.

Another study by Handayani et al. (2023) focused on BNCT dose analysis using the MCNP code for glioblastoma multiforme, a stage IV brain cancer that is extremely difficult to treat and typically occurs in the cerebral hemispheres. The findings indicated that BNCT holds strong potential for glioblastoma therapy, as it can deliver higher absorbed doses to tumor tissues while remaining relatively safe for surrounding normal tissues [14].

Building upon these previous studies, the present research aims to calculate and analyze the absorbed dose for each at-risk organ based on the total dose rate and irradiation time. In addition, this study explores variations in BNCT application for pediatric cases using Monte Carlo simulations. The absorbed dose values are then compared with acceptable threshold limits for at-risk organs to evaluate potential deterministic effects.

The research methodology employs Monte Carlo simulations using MCNP version 6.2 to model neutron interactions in a 10-year-old head and neck phantom. The 10-year-old pediatric model was selected to represent the age range at which RMS commonly occurs while providing anatomically accurate characteristics for dosimetric simulations. This selection also allows comparison with the 5-year-old model used in Syamputra et al. (2018) [13], thereby expanding the understanding of BNCT applications across different pediatric age groups.

METHODS

This study employed Monte Carlo simulations using MCNP version 6.2. A total of 10 million particle histories (10^7 NPS) were simulated, exceeding the minimum recommended range of 5,000-10,000 NPS as specified in the *MCNP User Manual*. This number was selected to ensure statistically reliable results. Simulation convergence was assessed by monitoring the ten statistical check parameters provided in the MNCP output file.

Three types of tallies were employed to calculate the parameters in this simulation. The F4 tally was used to determine neutron flux (thermal, epithermal, and fast) passing through the cells, the

F24 tally was utilized to measure the primary gamma dose rate, and the F34 tally was applied to assess the fast neutron dose rate. The results obtained from these three tallies were used as the basis for calculating the total dose rate, irradiation time, and absorbed dose for each organ.

The simulation was conducted using a 10-year-old pediatric phantom and a BNCT collimator. The phantom was based on the Oak Ridge National Laboratory–Medical Internal Radiation Dose (ORNL-MIRD) model, which was modified to include only the head and neck regions. This phantom comprises at-risk organs such as the brain, spinal cord, and thyroid.

Additionally, a spherical tumor geometry was modeled posterior to the brain and spinal cord, consisting of three target volumes: the Gross Tumor Volume (GTV) with a diameter of 1.5 cm, the Clinical Target Volume (CTV) with a diameter of 1.8 cm, and the Planning Target Volume (PTV) with 2 cm. The GTV and CTV materials were defined based on tumor tissue composition, whereas the PTV was modeled using normal tissue composition to represent the peripheral region adjacent to healthy tissue [15].

This assumption was applied solely for comparative dosimetric analysis between the target volumes and the Organs at Risk (OARs) and was not intended to represent the clinical definition of the PTV used in conventional radiotherapy planning. The head and neck phantom model is illustrated in Fig. 1.

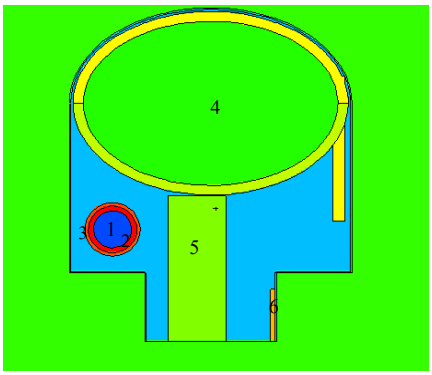

Fig. 1. Two-dimensional (2D) representation of the head and neck phantom used in the BNCT simulation.

Table 1. Composition of GTV material used in the MCNP simulation.

Atom	Code	Mass Fraction
H	1001	0.0989970
B	5010	0.000070
C	6012	0.2689919
N	7014	0.0449987
O	8016	0.5689829
P	15031	0.0179995

Numbers 1, 2, and 3 represent the GTV, CTV, and PTV, respectively. Number 4 corresponds to the brain, number 5 to the spinal cord, and number 6 to the thyroid. The visualization of the head and neck phantom was generated using Visual Editor version X_24E. The colors shown in Fig. 1 indicate different tissue types corresponding to the geometry of the head and neck phantom. The GTV, representing the tumor location, was defined based on the composition listed in Table 1 [13].

The BNCT collimator model used in this study was adopted from the previous work in Handayani et al. (2023) [15], with the neutron source originating from the Kartini Reactor. The collimator model consists of layered components and materials designed to generate a neutron beam within the epithermal energy range, suitable for therapeutic BNCT applications. The initial neutron source energy used in the simulation was 0.1 MeV, corresponding to the epithermal range.

The boron concentration was set to 70 µg/g of tumor tissue. The outputs from the MCNP 6.2 simulation included neutron flux, neutron dose rate, and primary gamma dose rate. The neutron flux data were subsequently used to calculate the alpha dose rate, proton dose rate, and secondary gamma dose rate, which were then used to determined the total dose rate, irradiation time, and absorbed dose.

The absorbed dose components in BNCT were calculated using the following equations [16]:

The boron (alpha) dose is generated from the capture reaction of thermal neutrons by the ^{10}B isotope, producing ^{7}Li and an alpha particle with a total energy release of 2.33 MeV. The alpha dose rate can be calculated using the following Eq. (1):

$$\dot{D}_B = \Phi_{Thermal}.N_B.\sigma_B.Q \quad (1)$$

where $\dot{D}_B$ is the boron dose rate (Gy/s), $\Phi_{Thermal}$ is the thermal neutron flux (n.cm^{-2}.s^{-1}), N_B is the number of boron atoms per kg of tissue (atoms/kg tissue), σ_B is the microscopic cross-section (barn), and Q is the particle energy (MeV).

The proton dose is generated from the neutron capture interaction of Boron with Nitrogen-14, which produces a proton with an energy of 0.66 MeV. The proton dose rate can be calculated using the following Eq. (2):

$$\dot{D}_p = \Phi_{Thermal}.N_N.\sigma_p.Q \quad (2)$$

where $\dot{D}_p$ is the proton dose rate (Gy/s), Φ_{Termal} is the thermal neutron flux in the tissue (n.cm^{-2}.s^{-1}), N_N is the number of nitrogen atoms per kilogram of

tissue (atoms/kg tissue), σ_p is the microscopic cross-section (barn), and Q is the particle energy (MeV).

Hydrogen atoms in tissue interact with thermal neutrons, producing gamma rays with an energy of 2.23 MeV. The gamma dose rate can be calculated using the following Eq. (3):

$$\ddot{R} = \Phi_{Thermal} . N_{i-tissue} . \sigma \quad (3)$$

wwhere $\ddot{R}$ is the gamma-ray release rate, $\Phi_{Thermal}$ is the thermal neutron flux in the tissue (n.cm^{-2}.s^{-1}), $N_{i-tissue}$ is the number of hydrogen atoms per kilogram of tissue (atoms/kg tissue), and σ is the microscopic cross-section (barn). The gamma dose rate can then be calculated using Eq. (4):

$$\dot{D}_\gamma = \ddot{R} . \Delta . \phi \quad (4)$$

where $\dot{D}_\gamma$ is the gamma dose rate (Gy/kg), $\ddot{R}$ is the gamma-ray release rate, Δ is the absorbed dose rate coefficient (Gy.kg/Bq.s), and ϕ is the absorbed dose fraction for gamma rays.

The total dose rate represents the sum of the alpha dose rate, proton dose rate, neutron scattering dose rate, and gamma dose rate, and can be expressed by the following Eq. (5):

$$\dot{D}_{total} = (W_\alpha . \dot{D}_\alpha) + (W_p . \dot{D}_p) + (W_n . \dot{D}_n) + (W_\gamma . \dot{D}_\gamma) \quad (5)$$

where $W_{particle}$ is the radiation quality factor, the values of which are listed in Table 2. The value of $\dot{D}_n$ is obtained by running the simulation input code.

The irradiation time is defined as the ratio between the minimum therapeutic dose required to eliminate cancer cells and the total dose rate. For pediatric rhabdomyosarcoma treated with BNCT, the therapeutic dose range is 36-50 Gy [13]. The irradiation time can be determined using the following Eq. (6):

$$t = \frac{D_{min}}{\dot{D}_{total}} \quad (6)$$

where t is the irradiation time (s), D_{min} is the minimum therapeutic dose (Gy), and $\dot{D}_{total}$ is the total dose rate (Gy/s).

Table 2. List of Radiation quality factors used in this study [17].

Radiation Source	Radiation Quality Factor
Boron	3.8
Proton	3.2
Neutron	3.2
Gamma	1.0

After determining the irradiation time, the absorbed dose received by each organ is calculated. The total dose must then be analyzed to ensure that the dose absorbed by healthy tissues or organs at risk (OARs) does not exceed their respective threshold limits. The absorbed dose can be calculated using the following Eq. (7):

$$D = \dot{D}_{total} \times t \quad (7)$$

where D is the absorbed dose (Gy), $\dot{D}_{total}$ is the total dose rate (Gy/s), and t is the irradiation time (s).

RESULTS AND DISCUSSION

The simulation was executed using Total Commander (64-bit) with a total of 1.0×10^7 particle histories (NPS). The statistical reliability of the simulation results was verified using the Tally Fluctuation Chart (TFC) feature available in MCNP version 6.2.

Based on the output of the three tallies (F4, F24, and F34), the relative errors were 0.168%, 0.632%, and 0.234%, respectively. These values are well below the 10% uncertainty limit recommended by the MCNP® User Manual. Furthermore, all three tallies exhibited high Figures of Merit (FOM) 1187.3 for F4, 249.1 for F24, and 706.6 for F34 indicating good statistical efficiency and convergence.

Evaluation of the ten statistical check parameters described in the MCNP® User's Manual (LA-UR-17-29981) revealed no oscillatory behavior, significant deviations, or inter-batch correlations. Therefore, the simulation results were confirmed to have achieved numerical convergence and statistical stability, ensuring that the outputs from the three tallies could be reliably used to calculate the total dose rate, irradiation time, and absorbed dose.

The resulting neutron flux, neutron dose rate, and primary gamma dose rate are summarized in Table 3.

Table 3. BNCT simulation output parameter measurements in the GTV.

Parameter	Output	Unit
Thermal neutron flux	5.22×10^9	n cm^{-2} s^{-1}
Epithermal neutron flux	1.22×10^{10}	n cm^{-2} s^{-1}
Fast neutron flux	5.91×10^7	n cm^{-2} s^{-1}
neutron dose rate	2.63×10^{-5}	Gy/s
Primary gamma dose rate	2.22×10^{-4}	Gy/s

The BNCT dose rate consists of four main components: the boron dose rate, proton dose rate, scattered neutron dose rate, and gamma dose rate. The alpha, proton, and secondary gamma dose rates were calculated using Eq. (1)-(4), whereas the scattered neutron and primary gamma dose rates were obtained directly from the simulation output. The resulting BNCT dose rate values are presented in Fig. 2.

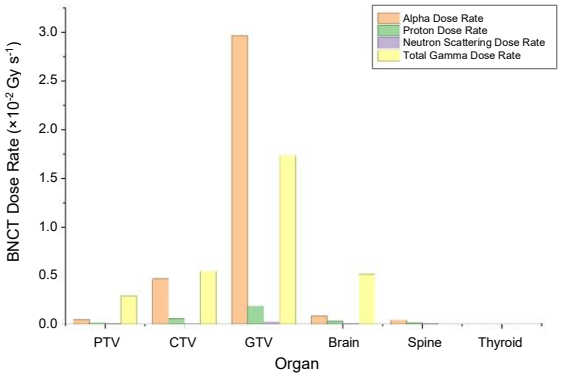

Fig. 2. BNCT dose rate for each component.

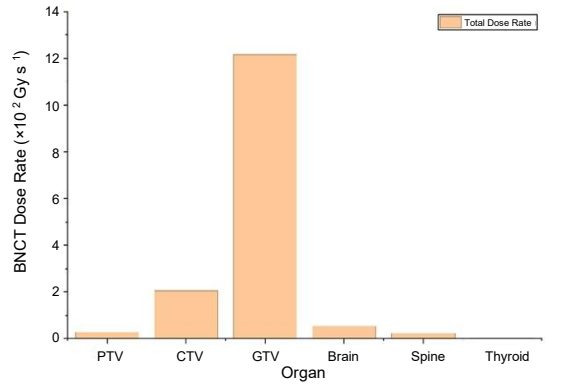

Fig. 3. Total dose rate for each organ.

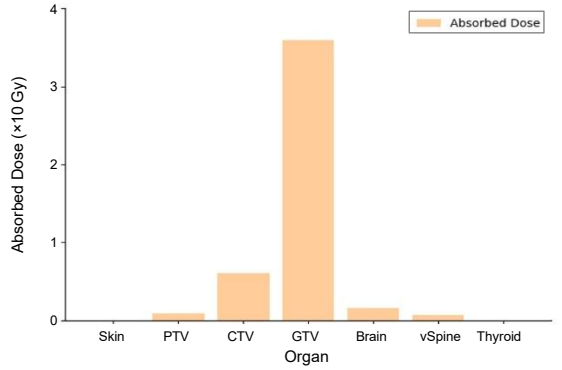

Fig. 4. Absorbed dose for each organ.

Table 4. Thermal neutron capture cross sections of constituent elements in the GTV.

Atom	σ (barn)
H	0.33
B	0.5
C	0.0035
N	0.08
O	0.00019
P	0.17

The highest BNCT dose rate was observed in the alpha component, which occurred within the GTV, followed by the CTV. The PTV and Organs at Risk (OARs) exhibited comparatively lower BNCT dose rates. This finding is consistent with previous studies [13,14], which also reported that the boron dose rate contributed the most to the total dose. The high boron dose rate is attributed to boron's exceptionally large thermal neutron capture cross section compared to other elements. The corresponding values are presented in Table 4 [18].

Boron, which possesses the highest neutron capture cross section among the constituent elements of tissue, has a greater likelihood of interacting with thermal neutrons. The thermal neutron capture reaction of boron generates lithium and alpha particles, both of which play a crucial role in the destruction of cancer cells. Consequently, the highest total dose rate was observed in the GTV, as shown in Fig. 3.

The total dose rate was calculated using Eq. (5). Based on this equation, the boron dose rate resulting from the (^{10}B (n,α)^{7}Li) reaction contributes the most significantly, as the radiation quality factor for the boron component is relatively high (3.8). Furthermore, the boron concentration in the GTV is the highest (100% of the administered boron concentration), leading to an increased reaction rate of (^{10}B) and, consequently, the highest local alpha dose. After determining the total dose rate, the irradiation time was calculated using Eq. (6), with a reference minimum therapeutic dose for pediatric rhabdomyosarcoma of 36 Gy [13].

The total dose rate used in this study corresponds to the GTV, with a value of 0.112267 Gy/s [13-15]. The irradiation time was calculated to be 296.33 seconds, equivalent to 4 minutes and 56.33 seconds. This irradiation duration is considerably shorter than that reported in previous studies, which were on the order of hours [13], and is comparable to other studies [14,15], which achieved irradiation times on the order of minutes. Subsequently, the absorbed dose in this study was determined by multiplying the total dose rate of each organ at risk by the irradiation time. The resulting absorbed dose values are presented in Fig. 4.

According to Fig. 4, the highest absorbed dose was observed in the GTV, where the cancerous tissue is located. The absorbed dose is primarily governed by the total dose rate, indicating that organs with higher total dose rates will consequently exhibit higher absorbed doses, as expressed in Eq. (7). However, the total dose rate is not the sole determining factor; the irradiation time also influences the absorbed dose in each organ in a

similar manner. Therefore, the distribution pattern presented in Fig. 3 closely resembles that shown in Fig. 2.

In radiation therapy, including BNCT, the absorbed dose within the GTV should be maximized, while the dose delivered to surrounding organs should be minimized to prevent unnecessary damage [19]. Although adjacent organs classified as organs at risk (OARs) receive relatively low doses, these organs may still experience certain biological effects [13-15]. One such effect is the deterministic effect, which occurs when radiation exposure exceeds a specific dose threshold. For instance, deterministic effects on the skin manifest as erythema at doses between 2 until 3 Gy, whereas the thyroid may develop hypothyroidism when the absorbed dose exceeds 5 Gy [14]. Based on the absorbed doses received by the skin and thyroid in this study, the occurrence of deterministic effects is expected to be minimal.

CONCLUSION

From this study, it can be concluded that the absorbed dose values received by the organs at risk namely, the skin, brain, spinal cord, and thyroid were 0.00641 Gy, 1.566 Gy, 0.710 Gy, and 0.018 Gy, respectively. Deterministic effects on the skin and thyroid were minimal, as the absorbed doses did not exceed their respective threshold limits.

ACKNOWLEDGMENT

The authors would like to thank the Dean of the Faculty of Science and Mathematics, Diponegoro University, for providing financial support through the Research Grant (Number: 25.VI.I/UN7.F8/PP/II/2024).

AUTHOR CONTRIBUTION

The first and third authors contributed to supervision and theoretical corrections. The second author contributed to the writing of the manuscript, while the fourth author contributed to the research methodology and administrative tasks.

REFERENCES

1. E. Setiyaningrum, Onkologi. Indomedia Pustaka, Sidoarjo (2018) 1. (in Indonesian)
2. E. R. Puteri and A. Rahman, Rhabdomyosarcoma Orbita, Jurnal Kesehatan Andalas **8** (2019) 743. (in Indonesian)
3. I. Dziuba, P. Kurzawa, M. Dopierala *et al*., Pol. J. Pathol. **69** (2018) 20.
4. L. Reniarti, N. Fatharani, and N. Suryawan, Althea Med. J. **7** (2020) 136.
5. D. Seneviratne, P. Advani, D. M. Trifiletti *et al*., Cancers **14** (2022) 3009.
6. P. Coghi, T. Fazal, N. S. Hosmane *et al*., Inorg. Chem. Commun. **159** (2024) 111698.
7. S. Namdev and G. Kaur, *A Mini Review on Application of Boron Neutron Capture Therapy in Cancer Treatment,* in: IOP Conf. Ser.: Mater. Sci. Eng. **1225** (2022) 012047.
8. S. G. Ntoy and Y. Sardjono, Jurnal Teknologi Reaktor Nuklir **19** (2017) 159. (in Indonesian)
9. G. Gambarini, D. Bettega, A. Gebbia *et al*., *BNCT Dosimetry: Peculiarities and Methods*, in: J. Phys.: Conf. Ser. **1154** (2019) 012008.
10. S. Choudhary, Cancer Ther. Oncol. Int. J. **12** (2018) 555834.
11. A. Wicaksono, Risalah Fisika **2** (2018) 21. (in Indonesian)
12. H. Park, H. Paganetti, J. Schuemann *et al*., Phys. Med. Biol. **66** (2021) 18TR01.
13. D. N. I. Syamputra, Y. Sardjono and R. S. N. Mahmudah, ASEAN J. Sci. Technol. Dev. **35** (2018) 235.
14. L. T. Handayani, W. S. Budi, and F. Arianto, Jurnal Fisika Unand (JFU) **12** (2023) 683. (in Indonesian)
15. N. Handayani, K. K. Soelistiyono and F. Arianto, Indones. J. Appl. Phys. **14** (2023) 176.
16. I. M. Ardana, A. D. Noerwasana, and Y. Sardjono, *Kajian Teknologi Boron Neutron Capture Therapy (BNCT) dan Aspek Regulasinya.* in: Prosiding Seminar Nasional Teknologi Energi Nuklir (2021) 95. (in Indonesian).
17. A. F. Harish, Warsono, and Y. Sardjono, ASEAN J. Sci. Technol. Dev. **35** (2018) 187.
18. S. F. Mughabghab, Thermal Neutron Capture Cross Sections, Resonance Integrals and G-Factors, INDC(NDS)-440, International Atomic Energy Agency (IAEA), Vienna (2003).
19. B. Poedjomartono, Y. Sardjono, E. Meiyanto *et al*., Atom Indones. **45** (2019) 139.